Heat Transfer by Thermals in the Convective Boundary Layer

U. Schumann and H. Schmidt

DLR, Institut für Physik der Atmosphäre,
D-8031 Oberpfaffenhofen, Fed. Rep. of Germany

1. Introduction

The convective boundary layer (CBL) develops in the atmosphere if turbulence generated by buoyancy due to upward heat flux from the surface dominates relative to turbulence generated by mean shear. The CBL extends from the surface up to an inversion layer at height z_i. Above the inversion, the fluid is stably stratified. Turbulence in the mixed layer below the inversion scales with the convective velocity $w_* = (g\,\beta\,z_i\,Q_s)^{1/3}$ and the convective temperature $T_* = Q_s/w_*$, where g, β, and Q_s are the gravitational acceleration, the volumetric expansion coefficient and the temperature flux at the surface, respectively. Typical values in the atmosphere are $z_i = 1000m$, $w_* = 1m/s$, $T_* = 0.1K$ and the related Rayleigh number is of the order 10^{18}, while previous laboratory experiments are limited to Rayleigh numbers less than about 10^9, e.g. see [1]. The surface layer ($0 \le z \le 0.1z_i$) is affected by the surface roughness height z_0, where z_i/z_0 is typically larger than 1000. The surface temperature θ_s exceeds the temperature θ_m of the mixed layer by an amount $\Delta\theta = \theta_s - \theta_m$ as a function of T_* and z_i/z_0.

If the mean horizontal wind speed $\overline{u}(z)$ is nonzero then the surface layer can be described using the Monin-Obukhov (M-O) similarity theory [7]. This theory relates the mean wind and mean temperature profiles to the surface friction velocity and the corresponding friction temperature scales $u_* = (-\overline{\tau}_s/\rho)^{1/2}$, $\theta_* = -Q_s/u_*$, where $\overline{\tau}_s/\rho = \overline{(w'u')}_s$ is the turbulent momentum flux close to the surface. As has been recognized by Businger [2], the M-O-theory breaks down in the windless case. However, when $\overline{u} = 0$ and consequently $u_* = 0$ there are still substantial convective motions near the surface. This convective motions introduce a shear production of turbulence, and, hence, locally a friction velocity $\tilde{u}_*$ may be defined.

In this study, we determine the coherent spatial structure of the turbulent motion field in the CBL and the heat transfer for the case of zero mean wind and uniform surface properties. For this purpose, we have performed a large eddy simulation (LES) of the CBL in a domain of size $5z_i \cdot 5z_i \cdot 1.5z_i$ using $160 \cdot 160 \cdot 48$ grid cells with respect to the two horizontal and the vertical coordinates, respectively. The method has been described in [14] and verified by comparison with the experiments of Deardorff & Willis [6]. The details of the subgrid-scale model and comparisons with further experiments are reported in [11 and 12]. The heat transfer results are compared with the predictions of a simple model [13] which is based on the coherent thermal structure. Since the details are fully described in [11 and 12], this paper summarizes the results on the structure of thermals, includes the mean values of updrafts and downdrafts, and compares the heat transfer results with earlier predictions.

Advances in Turbulence 2
Editors: H.-H. Fernholz and H.E. Fiedler

2. Coherent structure in the CBL

The simulation results show that the convection in the lower 40 % of the CBL assumes a non-steady spoke pattern, see Fig. 1, as found earlier in laboratory experiments by Busse & Whitehead [4] and Willis & Deardorff [15] for much lower Rayleigh numbers. Also Mason [10] found the spoke pattern in a LES but with less resolution and larger eddy diffusivities. In the main portion of the mixed layer strong updrafts in narrow columns of relatively warm fluid are surrounded by larger areas of slowly sinking motion. The area fraction and mean velocities in the updrafts and downdrafts are shown in Fig. 2. This information is of importance in modeling turbulent transports across the mixed layer [5].

The ensemble mean structure of the updrafts has been determined by conditional sampling. Let (x_i, y_i), $i = 1,2,...,n$, be the horizontal coordinates of a centre of an updraft and $f(x, y, z, t)$ be any component of the flow field. Then the conditional average $\tilde{f}$ is the mean value

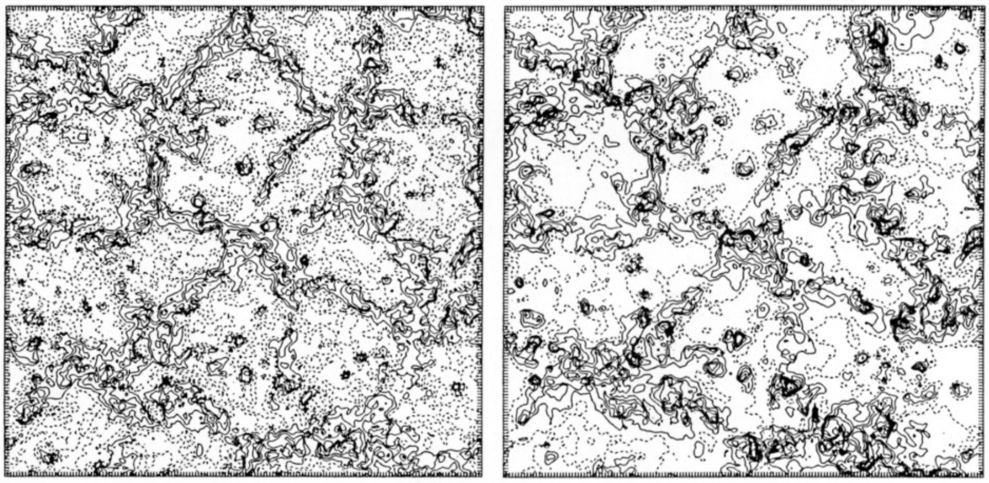

Fig. 1. Horizontal cross-section showing spoke-pattern convection in terms of contour lines of vertical velocity (left) and temperature fluctuations (right) at height $z/z_i = 0.25$. (The coordinates are x and y and the domain size is $5z_i \cdot 5z_i$.)

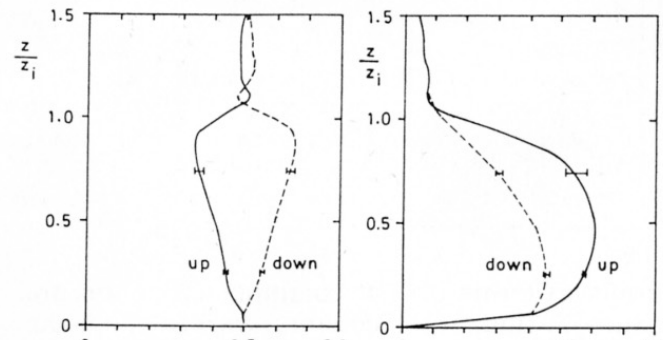

Fig. 2. Mean area fraction of updrafts (full curve) and downdrafts (dashed) and mean vertical velocities within these areas. The error bars indicate the scatter of the results within $6 \leq tw_*/z_i \leq 8$.

$$\tilde{f}(x, y, z, t) = \frac{1}{n} \sum_{i=1}^{n} f(x_i + x, y_i + y, z, t). \tag{1}$$

The coordinate values $x_i + x$ and $y_i + y$ are evaluated modulo $5z_i$, the periodicity length of the computational domain. The updraft's centres (x_i, y_i) are those positions where the vertical velocity for $z = z_c = 0.5\, z_i$ assumes a local maximum relative to all competing updrafts within a circle of radius z_i. Figure 3 shows the resultant mean values for various field components $\tilde{f}$ in a vertical plane through the axis of the mean updraft.

The results clearly show the existence of large-scale convective circulations which extend from the surface up to the inversion while scaling with z_i also in the lateral directions. The updrafts speed up to 2.0 w_* and are correlated with strong horizontal velocities in the surface layer (up to 0.36 w_*) and just below z_i. This large-scale structure is superposed by updrafts with relative small radius of coherence causing local maxima of all quantities shown in Fig. 3 near the refer-

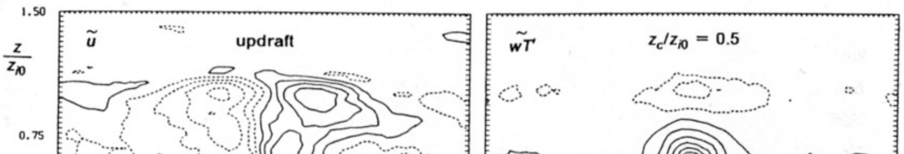

Fig. 3. Conditionally averaged updrafts in terms of (left column:) horizontal and vertical velocity $\tilde{u}$ and $\tilde{w}$, temperature $\tilde{T}$, and (right column:) vertical heat flux $\widetilde{w'T'}$, momentum flux $\widetilde{u'w'}$, and pressure fluctuation $\tilde{p}'$, in a vertical x-z plane. The contour line increments, the minimum and the maximum values are for the left column: (0.05, −0.36, 0.33)w_*, (0.2, − 0.1, 2.0)w_*, (0.3, −3., 2.7)T_*, from top to bottom panel; the corresponding values for the right column are (0.3, −0.3, 5.7)$w_* T_*$, (0.02, − 0.11, 0.16)w_*^2, (0.02, −0.17, 0.07)ρw_*^2, from top to bottom panel, respectively.

ence level. This fact is corroborated by conditional averages of local time derivatives of vertical velocity and temperature which indicate that thermals are rising like bubbles inside quasi-stationary plumes. Also a movie film of the computational results supports this interpretation. At larger distances from the point of reference, the accelerations are small. The small time-derivatives of horizontal motion in the surface layer confirms the applicability of the M-O relationships for evaluation of surface-fluxes. This justifies the use of the M-O-boundary condition in the model [13].

Above the reference height z_c the motion is away from the updrafts and possesses two maxima of the horizontal velocity, one just above the reference level ($\tilde{u}/w_* = 0.15$) and a second near the inversion ($\tilde{u}/w_* = 0.2$). The first maximum is due to bubbles in the updrafts which displaces fluid sideways while rising. The upper maximum reflects the large-scale coherent motion. Temperature fluctuations are - besides the maximum near z_c - still quite large near the surface. This phenomenon is characteristic for plumes extending from the surface far up into the mixed layer. Due to the stable stratification in the interfacial layer the updrafts cause negative temperature fluctuations ($-1.9\ T_*$) above $0.8 z_i$.

Figure 3 also shows the fluxes $\widetilde{wT'}$ and $\widetilde{u'w}$ and the dynamic pressure fluctuations $\tilde{p}'$ connected with updrafts. Updrafts induce large values of upward heat flux which by far exceed the average values. Updrafts are also connected with significant amounts of momentum fluxes. Most of these fluxes are simply due to the product $\tilde{u}\tilde{w}$ but small-scale turbulence (at resolved and subgrid scales) also contributes to these fluxes. Note that the momentum flux is virtually zero at the surface itself. Thus friction at the surface plays a minor role for the dynamics of the updrafts. This result was postulated in [13] where it was assumed that the horizontal motion in the surface layer loses most of its momentum by large-scale advection across the interface between surface layer and mixed layer.

The pressure signal exhibits considerable statistical uncertainty but it is nevertheless obvious that the pressure is most affected by the large-scale dynamics of the updrafts. The negative pressure fluctuation just below the point of reference presumably is caused by buoyant bubbles which suck in air from below and from the sides. Pressure fluctuations assume a positive maximum near the inversion presumably because of pressure head due to thermals impinging on the inversion. The hydrostatic pressure $\tilde{p}_h$, plotted in [12], shows large negative values at the surface below the relatively light updraft ($\tilde{p}_h(0,0,0) = -0.9\ \rho w_*^2$). For comparison the actual pressure field $\tilde{p}'$ connected with the updraft, see Fig. 2, is much smaller in amplitude (factor 6.7) and different in shape. Thus, hydrostatic pressure is a poor estimate for the actual pressure in the CBL. Obviously, the main portion of buoyancy forces is balanced by inertia forces and entrainment drag rather than by pressure. However, the actual pressure fluctuations and the hydrostatic pressure both have the tendency to drive horizontal motions from the foot of downdrafts towards the foot of updrafts as assumed in the model [13]. The smaller pressure forces are balanced by smaller momentum fluxes.

3. Heat transfer as a function of surface roughness

The LES results are applied to investigate how surface roughness influences the minimum friction velocity and the heat transfer at the surface. The concept of minimum friction velocity was introduced by Businger [2]. Note that the friction velocity is zero in the ensemble mean. We define the minimum friction velocity $\tilde{u}_*$ as the rms value of friction velocity at the surface for zero mean wind. The heat transfer is measured in terms of the difference $\Delta\theta$ between the mean temperature θ_s at the surface ($z = z_0$) and $\theta_m = \overline{T}(0.1z_i)$ at the top of the surface layer. Both values are computable from the LES where local values of friction and temperature differences are computed by locally applying the M-O-relationships. Schumann [13] found that these quantities are smooth functions of $\ln(z_i/z_0)$ and approximately equal to

$$\frac{\tilde{u}_*}{w_*} = 0.52\left(\frac{z_0}{z_i}\right)^{1/6}, \quad \frac{\Delta\theta}{T_*} = \left(10\,\frac{z_i}{z_0}\right)^{1/3}, \text{ for } 10^2 < \frac{z_i}{z_0} < \left(\frac{Ra}{560}\right)^{3/8} \tag{2}$$

in air. Here $Ra = (\beta\, g\, \Delta\theta\, z_i^3)/(\nu\, \mu)$ is the Rayleigh number (ν, μ are the diffusivities for momentum and heat, respectively).

In Fig. 4 we have plotted the prediction of Schumann [13] (full curves) and his approximation reported in eq. (2) (dashed lines). The symbols for three values of the surface roughness represent the results of the LES. We find that the LES-results agree very well with the predictions and do support the model's results. In particular, the LES-results corroborate the curved trend shown by the full curves.

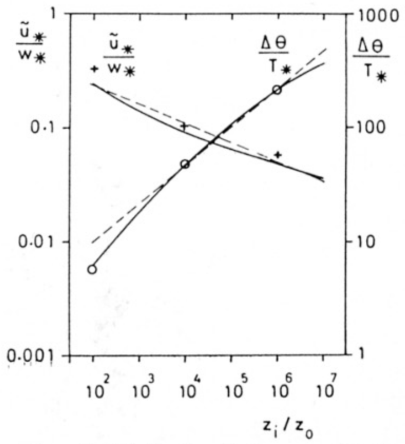

Fig. 4. Plot of minimum friction velocity $\tilde{u}_*$ over the convective velocity scale w_* and of the temperature difference $\Delta\theta$ over the convective temperature scale T_* versus the boundary layer/roughness height ratio z_i/z_0. The full curves correspond to the model prediction [13] and the dashed represent approximative power laws. The crosses and circles are the LES-results for $\tilde{u}_*$ and $\Delta\theta$, respectively.

4. Discussion

Only few data are available from measurements to validate the theoretical results. Frisch & Businger [8] measured $\Delta\theta \cong 13$ K. Unfortunately, their paper does not contain all the scales necessary to test the theoretical prediction. However, Businger (personal communication, 1988) estimates 8 K $< \Delta\theta <$ 15 K, 0.09 K $< T_*$ $<$ 0.13 K, 750 m $< z_i <$ 1500 m, and 1 cm $< z_0 <$ 2 cm. These data define a box $60 < \Delta\theta/T_* < 170$, $4 \cdot 10^4 < z_i/z_0 < 15 \cdot 10^4$, which is crossed by the line predicted by eq. (2) which provides at least some verification.

In terms of the common Nusselt and Prandtl numbers, $Nu = Q_s z_i/(\mu\Delta\theta)$, $Pr = \nu/\mu$, and the Rayleigh number defined above, the heat transfer relationship can be expressed as

$$Nu = F \cdot (Ra\,Pr)^{1/2}, \quad F = \left(\frac{T_*}{\Delta\theta}\right)^{3/2}, \quad F \cong \left(\frac{z_0}{10\,z_i}\right)^{1/2}, \tag{3}$$

where eq. (2) is being used to obtain the approximation for $F = F\,(z_i/z_0)$. This result differs essentially from previous laboratory results, see e.g. [1], which predict $Nu \sim Ra^{1/3}$. Schumann [13] identified the limited Rayleigh-numbers of these experiments as the reason for this difference. Our result has been deduced for a rough surface. In order to be classified as rough, the ratio z_i/z_0 must be small as stated in eq. (2). It requires, e.g., $Ra > 5.6 \cdot 10^{10}$ for $z_i/z_0 = 1000$, and even larger Rayleigh numbers if the height-ratio increases. Hence, previous measurements apply for effectively smooth surfaces and further experiments are desirable to verify the results (2) and (3). It is therefore reassuring to note that Kraichnan [9] deduced theoretically $Nu \sim Ra^{1/3}$ for convection over smooth surfaces as long as the viscous/conductive sublayer limits the heat transfer at moderate Rayleigh numbers but $Nu \sim Ra^{1/2}$ for very large Rayleigh numbers as they arise in atmospheric boundary layers. For $z_i/z_0 > 1035Pr/10$, our result is also consistent with the upper bound $Nu < (Ra/1035)^{1/2}$ derived by Busse [3] for smooth surfaces. (The exact numerical value applies to Rayleigh-Benard convection). It implies $\Delta\theta/T_* > 4.6$. As can be seen from Fig. 4, this limit is reached for low values of z_i/z_0 where the validity of eq. (2) ends. Hence, the coherent structure of the CBL is close to optimal in transporting heat.

References

1 R.J. Adrian, R.T.D.S. Ferreira, T. Boberg: Experim. in Fluids 4, 121 (1986)
2 J.A. Businger: Bound.-Layer Meteorol. 4, 323 (1973)
3 F.H. Busse: J. Fluid Mech. 37, 457 (1969)
4 F.H. Busse, J.A. Whitehead: J. Fluid Mech. 66, 67 (1974)
5 R.B. Chatfield, R.A. Brost: J. Geophys. Res. 92, D11, 13263 (1987)
6 J.W. Deardorff, G.E. Willis: Bound.-Layer Meteorol. 32, 205 (1985)
7 A.J. Dyer: Bound.-Layer Meteorol. 7, 363 (1974)
8 A.S. Frisch, J.A. Businger: Bound.-Layer Meteorol. 3, 301 (1973)
9 R.H. Kraichnan: Phys. Fluids 5, 1374 (1962)
10 P.J. Mason: J. Atmos. Sci, in press (1989)
11 H. Schmidt: DFVLR-FB-88-30 (1988)
12 H. Schmidt, U. Schumann: J. Fluid Mech., in press (1989)
13 U. Schumann: Bound.-Layer Meteorol. 44, 311 (1988)
14 U. Schumann, T. Hauf, H. Höller, H. Schmidt, H. Volkert: Beitr. Phys. Atmosph. 60, 413 (1987)
15 G.E. Willis, J.W. Deardorff: J. Geophys. Res. 84, C1, 295 (1979)